[CANCER RESEARCH 60, 5074–5079, September 15, 2000]

Human Cytochrome P450 CYP2A13: Predominant Expression in the Respiratory Tract and Its High Efficiency Metabolic Activation of a Tobacco-specific Carcinogen, 4-(Methylnitrosamino)-1-(3-pyridyl)-1-butanone[1]

Ting Su, Ziping Bao, Qing-Yu Zhang, Theresa J. Smith, Jun-Yan Hong,[2] and Xinxin Ding[2]

Wadsworth Center, New York State Department of Health, Albany, New York 12201 [T. S., Q-Y. Z., X. D.]; School of Public Health, State University of New York at Albany, Albany, New York [T. S., X. D.]; and Environmental and Occupational Health Sciences Institute, University of Medicine and Dentistry of New Jersey, Piscataway, New Jersey 08854 [Z. B., T. J. S., J-Y. H.]

ABSTRACT

The human *CYP2A* subfamily comprises three genes, *CYP2A6*, *CYP2A7*, and *CYP2A13*. CYP2A6 is active toward many carcinogens and is the major coumarin 7-hydroxylase and nicotine C-oxidase in the liver, whereas CYP2A7 is not functional. The function of CYP2A13 has not been characterized. In this study, a CYP2A13 cDNA was prepared by RNA-PCR from human nasal mucosa and was translated using a baculovirus expression system. In a reconstituted system, the expressed CYP2A13 was more active than CYP2A6 in the metabolic activation of hexamethylphosphoramide, *N*,*N*-dimethylaniline, 2′-methoxyacetophenone, and *N*-nitrosomethylphenylamine but was much less active than CYP2A6 in coumarin 7-hydroxylation. Of particular interest, CYP2A13 was highly active in the metabolic activation of a major tobacco-specific carcinogen, 4-(methylnitrosamino)-1-(3-pyridyl)-1-butanone, with a catalytic efficiency much greater than that of other human cytochrome P450 isoforms examined previously. The tissue distribution of CYP2A13 was determined with isoform-specific RNA-PCR. CYP2A13 mRNA was detected in liver and a number of extrahepatic tissues, including nasal mucosa, lung, trachea, brain, mammary gland, prostate, testis, and uterus, but not in heart, kidney, bone marrow, colon, small intestine, spleen, stomach, thymus, or skeletal muscle. Quantitative PCR analysis further revealed that CYP2A13 mRNA is expressed at the highest level in the nasal mucosa, followed by the lung and the trachea. Together, these findings suggest that CYP2A13 plays important roles in xenobiotic toxicity and tobacco-related tumorigenesis in the human respiratory tract.

INTRODUCTION

Three members of the *CYP*[3]*2A* gene subfamily, *CYP2A6*, *CYP2A7*, and *CYP2A13*, have been identified in humans (1). CYP2A6 constitutes ~1–10% of the total microsomal CYP in human liver (2, 3) and has also been detected in human nasal mucosa (4–7) and lung (8–10). CYP2A6 is the major coumarin 7-hydroxylase (compare Ref. 11) and nicotine C-oxidase in human liver microsomes (12, 13). The other known substrates for CYP2A6 include many toxicants and carcinogens, such as aflatoxin B1, NNK, *N*-nitrosodiethylamine, *N*-nitrosonornicotine, DCBN, and hexamethylphosphoramide (6, 11, 14, 15). Deletion of the *CYP2A6* gene has been found to correlate with reduced lung cancer risk (16).

CYP2A7 was first cloned from a hepatic cDNA library (17). However, heterologously expressed CYP2A7 showed no catalytic activity (17, 18). CYP2A13 cDNA has not been isolated previously; the reported protein sequence was deduced from the predicted coding region of a *CYP2A13* genomic clone (1). On the basis of its sequence features that resemble the nonfunctional CYP2A7 and CYP2A6v1 (a genetic variant of CYP2A6) proteins, the CYP2A13 protein was predicted to be nonfunctional in coumarin 7-hydroxylation (1). Because the deduced amino acid sequence of CYP2A13 shares a 95.4% identity with that of CYP2A6 (1), antibodies and chemical probes for CYP2A6 may interact with CYP2A13. Therefore, CYP2A13 may confound results obtained in studies on CYP2A6.

The tobacco-specific nitrosamine, NNK, which is formed from the nitrosation of nicotine during tobacco processing and cigarette smoking, has been suggested to play an important role in human tobacco-related cancers (19, 20). NNK induces lung tumors in all laboratory animals tested as well as nasal cavity, pancreatic, and liver tumors in rats (19, 20). In order for NNK to exert its carcinogenicity, it must be metabolically activated. The metabolic activation of NNK involves α-hydroxylation of the methyl or methylene carbon, leading to the formation of electrophiles, which can pyridyloxobutylate and methylate DNA, respectively (20). Hydroxylation at the methyl position leads to the formation of formaldehyde and 4-(3-pyridyl)-4-oxobutyldiazohydroxide; the latter decomposes to form 4-hydroxy-1-(3-pyridyl)-1-butanone (keto alcohol). Hydroxylation at the methylene carbon of NNK leads to the formation of 4-oxo-1-(3-pyridyl)-1-butanone (keto aldehyde) and methyldiazohydroxide. The detectable products for the two activation pathways are keto alcohol and keto aldehyde.

It is well-documented that CYP enzymes catalyze the activation of NNK (21–25). Of the human CYPs examined, CYP1A1, CYP2A6, CYP2D6, CYP2E1, and CYP3A4 catalyzed the formation of keto aldehyde, and CYP1A1, CYP1A2, CYP2A6, CYP2B6, CYP2D6, CYP2E1, CYP2F1, and CYP3A4 had activity in the formation of keto alcohol (21–25). Although some of the CYPs display activity in the formation of both keto aldehyde and keto alcohol, the CYP enzymes generally show predominance for one activation pathway over the other. Thus, CYP1A1, CYP2A6, and CYP3A4 have higher activity for keto aldehyde formation, whereas CYP2D6 and CYP2E1 are more selective for keto alcohol formation (21–25). When one considers the kinetic properties of the various CYPs, CYP2A6 and CYP1A2 have the lowest K_m (120 and 300 μM, respectively) and relatively high V_{max} values for the formation of keto aldehyde and keto alcohol, respectively (21, 23, 25). Because human individuals are exposed to relatively low levels of NNK, the metabolic activation of this carcinogen appears to be more likely catalyzed by CYP2A6 and CYP1A2. However, the contribution of these and other CYP enzymes to NNK activation in human target tissues will be dependent both on their metabolic efficiency and their abundance in a given tissue.

In the present study, a CYP2A13 cDNA was cloned from human nasal mucosa, and its sequence was compared with the published *CYP2A13* genomic sequence (1). CYP2A13 protein was obtained by heterologous expression in insect cells and characterized. The tissue distribution of CYP2A13 was also determined by isoform-specific

Received 2/3/00; accepted 7/20/00.

The costs of publication of this article were defrayed in part by the payment of page charges. This article must therefore be hereby marked *advertisement* in accordance with 18 U.S.C. Section 1734 solely to indicate this fact.

[1] Supported in part by Public Health Service Grants ES07462 (to X. D.) and ES10048 (to J-Y. H.) from the NIH.

[2] To whom requests for reprints should be addressed, at (for J-Y. H.) Environmental and Occupational Health Sciences Institute, University of Medicine and Dentistry of New Jersey, 170 Frelinghaysen Road, Piscataway, NJ 08854-8020. Phone: (732) 445-7047; Fax: (732) 445-0119; E-mail: jyhong@rci.rutgers.edu; or (for X. D.) Wadsworth Center, New York State Department of Health, Empire State Plaza, Box 509, Albany, NY 12201-0509. Phone: (518) 486-2585; Fax: (518) 486-1505; E-mail: xding@wadsworth.org.

[3] The abbreviations used are: CYP, cytochrome P450; b_5, cytochrome b_5; DCBN, 2,6-dichlorobenzonitrile; NNK, 4-(methylnitrosamino)-1-(3-pyridyl)-1-butanone; MTBE, methyl *tert*-butyl ether; HPLC, high performance liquid chromatography; RT, reverse transcription.

RNA-PCR. We report here that CYP2A13 is highly active toward NNK and several other carcinogens and toxicants and that it is predominantly expressed in the human respiratory tract.

MATERIALS AND METHODS

Human Tissues and RNA Preparations. Total RNA samples isolated from the following human tissues, pooled from various numbers of subjects (*n*), were obtained from Clontech (Palo Alto, CA): liver ($n = 2$; ages 15 and 35), lung ($n = 5$; ages 14–40), trachea ($n = 84$; ages 17–70), kidney ($n = 8$; ages 24–55), heart ($n = 12$; ages 19–50), brain ($n = 2$; ages 16 and 36), mammary gland ($n = 8$; ages 23–47), prostate ($n = 23$; ages 26–64), testis ($n = 25$; ages 28–64), uterus ($n = 10$; ages 15–77), bone marrow ($n = 3$; ages 24–59), colon ($n = 2$; ages 35 and 50), small intestine ($n = 11$; ages 15–60), spleen ($n = 5$; ages 22–48), stomach ($n = 15$; ages 23–61), thymus ($n = 13$; ages 17–37), and skeletal muscle ($n = 10$; ages 23–56). All tissues were collected from nondiseased Caucasian individuals whose cause of death was trauma. RNAs of nasal turbinates and additional liver and lung RNAs were isolated from individual subjects, including three nasal tissues (ages 52–60; Caucasian; cause of death was heart failure) and one transplant donor lung tissue (age 53; Caucasian; cause of death was trauma) provided by the International Institute for the Advancement of Medicine (Exton, PA); two pulmonary samples prepared from resected normal lung tissues of subjects with lung tumor (ages 54 and 64; Caucasian) provided by Dr. Simon Spivack of the Wadsworth Center; and three hepatic tissues from transplant donor liver tissues (one 58-year-old Caucasian; two adults of unknown age or ethnicity) provided by Dr. Robert Jansing of the Wadsworth Center. The quality of each RNA sample was examined by electrophoretic analysis of 2 μg of RNA on a denaturing gel. Ethidium bromide staining of the gel detected distinct 28S and 18S rRNA bands with a intensity ratio of at least 1.5 (28S:18S). The UV absorbance ratio (260 nm/280 nm) was at least 1.8 for all RNA samples. The efficiency of RNA recovery for the prepared samples was about 6–10 μg/mg of liver, 1.5 μg/mg of lung, and 1–3 μg/mg of nasal mucosa.

Cloning of the Coding Region of CYP2A13 cDNA. PCR primers (forward primer: 5′-tcccatggccaccatgctg-3′; reverse primer: 5′-tcgctcagcggggcaggaag-3′) were designed according to the *CYP2A13* gene sequence (1); the underlined nucleotides represent translation initiation and termination codons, respectively. First-strand cDNA was synthesized by RT from 2 μg of human nasal mucosal total RNA with use of Moloney murine leukemia virus reverse transcriptase (Promega; Madison, WI) and an oligo $d(T)_{16}$ primer (Perkin-Elmer; Foster City, CA). The cDNA was amplified by high fidelity PCR using PfuTurbo DNA polymerase (Stratagene, La Jolla, CA) and cloned into pCR-Script vector (Stratagene) for sequence analysis. Nucleotide sequence was determined with vector primers and by primer walking with an automated DNA sequencer from Applied Biosystems (Model 373A) at the Molecular Genetics Core of the Wadsworth Center. Each position was analyzed at least three times in each orientation.

Heterologous Expression of CYP2A13 cDNA. The 5′-primer used for amplifying the CYP2A13 cDNA sequence contained an in-frame upstream ***ATG*** codon, which is undesirable for heterologous expression because it may introduce three extra amino acid residues at the amino terminus. This upstream ***ATG*** codon was later found to be ***ACT*** in all (>10) individuals genotyped and may represent additional errors in the original published genomic sequence (data not shown). One of the three cDNA clones sequenced had lost the first five bases in the 5′-primer during ligation into the pCR-Script vector. The resulting insert began with the ***TG*** in the upstream ***ATG*** codon, and the 3′-primer was intact. Therefore, this clone was used for heterologous expression.

The CYP2A13 cDNA insert was excised from the pCR-Script vector and inserted into the multiple cloning site of the baculovirus expression vector pVL1392 (PharMingen, SanDiego, CA). The integrity of the cloning sites was confirmed by sequencing. Recombinant viruses were made by cotransfecting the transfer plasmid and linearized BaculoGold viral DNA (PharMingen) into insect Sf9 cells. Detailed procedures for preparation and titering of virus stocks and detection of CYP expression have been described recently for the expression of CYP2A3 and CYP2A6 (14). The cells were harvested at 72 h postinfection, washed with PBS, and resuspended in 100 mM Tris-acetate buffer (pH 7.4) containing 1 mM EDTA and 150 mM potassium chloride. Microsomal fractions were prepared as described previously (14) and stored at −85°C until use.

Determination of Catalytic Activities. The contents of reaction mixtures are described in the table legends. The enzyme activities were found in preliminary studies to be linear with CYP concentrations under the conditions used. The rates of product formation were corrected for zero-time blanks that were quenched before the addition of NADPH. Formaldehyde formed from hexamethylphosphoramide, 2′-methoxyacetophenone, *N,N*-dimethylaniline, and *N*-nitrosomethylphenylamine was measured according to the method of Nash (26), and 7-hydroxylation of coumarin was assayed according to the method of Greenlee and Poland (27), with use of a Model LS50B Luminescence Spectrometer (Perkin-Elmer). Formation of the DCBN-protein adduct was assayed as described recently (28) with the use of 2,6-[ring-^{14}C]DCBN (16.7 Ci/mol, Sigma; St. Louis, MO) as a substrate. Formation of acetaldehyde from *N*-nitrosodiethylamine was assayed using HPLC after derivatization with 2,4-dinitrophenylhydrazine (29). MTBE metabolism was assayed by measuring *tert*-butyl alcohol formation by gas chromatography (30, 31).

For NNK metabolism, [5-^{3}H]NNK (2.4 Ci/mmol; purity >97%) and unlabeled NNK were purchased from Chemsyn Science Laboratories (Lenexa, KS). The radiolabeled NNK was further purified by reverse-phase HPLC before use. Authentic NNK metabolite standards were kindly provided by Dr. Stephen Hecht (University of Minnesota Cancer Center, Minneapolis, MN). Unless otherwise specified, incubation mixtures consisted of 100 mM sodium phosphate (pH 7.4), 1 mM EDTA, 3 mM $MgCl_2$, an NADPH-generating system (5 mM glucose 6-phosphate, 1 mM $NADP^+$, and 1.5 units of glucose 6-phosphate dehydrogenase), 10 μM NNK (containing 1 μCi [5-^{3}H]NNK), 5 mM sodium bisulfite, and 10 pmol of CYP2A13 or 20 pmol of CYP2A6 in a total volume of 0.4 ml. When b_5 was added, the molar ratio of CYP:b_5 was 1:4. Reactions were carried out at 37°C for 15 min and terminated with 50 μl each of 25% zinc sulfate and saturated barium hydroxide. The samples were centrifuged and filtered, and 50–200-μl aliquots were coinjected with 5 μl of NNK metabolite standards onto a reverse-phase HPLC system equipped with a Radioflow Detector (Radiomatic, Tampa, FL; Ref. 32). The HPLC conditions used were the same as previously described (33). The identity of the keto aldehyde and keto alcohol peaks was confirmed with two different HPLC conditions, in the presence and absence of sodium bisulfite. For kinetic studies, NNK concentrations of 2–160 μM were used in the incubations.

RNA-PCR Analysis of CYP2A13 Tissue Distribution. RNA-PCR was carried out with a set of CYP2A13-specific primers (forward primer: 2A13E6F1, 5′-caccctgcgctacggtttcc-3′; reverse primer: 2A13E9R1, 5′-gtcgatatccttaggcgactgagg-3′). The expected product (923–1416 in the coding region) is 494 bp in length. RT reaction was performed as described above. PCR mixtures contained 1× reaction buffer (Perkin-Elmer), 2 mM $MgCl_2$, 0.4 mM dNTPs, 5 μM of each primer, 2.5 μl of a RT mixture, and 1.25 units of Taq DNA polymerase in a total volume of 25 μl. PCR was performed using a two-step protocol (30 s at 94°C; 45 s at 68°C) for 35 cycles. PCR products were analyzed on agarose gels and visualized by staining with ethidium bromide.

Quantitative Analysis of CYP2A13 and CYP2A6 mRNA Levels by Competitive RNA-PCR. CYP2A13 and CYP2A6 PCR-mimics were prepared using a kit from Clontech. Competitive RNA-PCR was performed according to a protocol from Ambion (Austin, TX), using the same two-step protocol as described above for 35 cycles with a constant amount of RT reaction mixtures (2.5 μl) and serial dilutions of a PCR-mimic. The equality of the amounts of total RNA from different tissues used for RT was confirmed by determining the level of cyclophilin mRNA in each RNA sample by competitive RNA-PCR with a RT-Check kit from Ambion. Isoform-specific PCR primers used for amplification of CYP2A13 and the CYP2A13-mimic were the same as described above. The primers for amplification of CYP2A6 and the CYP2A6-mimic (forward primer: 5′-gggccaagatgccctacatg-3′; reverse primer: 5′-cgtcaatgtccttaggtgactgg-3′) were designed according to the CYP2A6 cDNA sequence (17). Ethidium bromide-stained PCR products were quantified by a Molecular Dynamics Model 595 Fluorimager at the Molecular Immunology Core of the Wadsworth Center. The levels of CYP2A13 or CYP2A6 mRNAs in different human tissues were calculated by extrapolating from the amounts of the PCR-mimics used in PCR reactions that generated products with equal intensity of the PCR-mimic band (CYP2A13-mimic: 622 bp; CYP2A6-mimic: 443 bp) and the CYP2A band (CYP2A13: 494 bp; CYP2A6: 381 bp).

```
                                        I4
                                        ↓
cDNA ...LLRMMLGSFQFTATSTGQLYEMFSSVMKHLPGPQQQAFKELQGLEDFIAK 250
gene             R   G
                                            I5
                                            ↓
cDNA     KVEHNQRTLDPNSPRDFIDSFLIRMQEEEKNPNTEFYLKNLVMTTLNLFF 300
gene
                                    I6
                                    ↓
cDNA     AGTETVSTTLRYGFLLLMKHPEVEAKVHEEIDRVIGKNRQPKFEDRAKMP 350
gene
                                                        I7
                                                        ↓
cDNA     YTEAVIHEIQRFGDMLPMGLAHRVNKDTKFRDFFLPKGTEVFPMLGSVLR 400
gene                                                     E
                                                    I8
                                                    ↓
cDNA     DPRFFSNPRDFNPQHFLDKKGQFKKSDAFVPFSIGKRYCFGEGLARMELF 450
gene               Q CS      E
```

Fig. 1. Deduced amino acid sequence of CYP2A13 cDNA and differences from the published *CYP2A13* gene sequence (1). The protein sequence deduced from CYP2A13 cDNA (*cDNA*) is shown on *top* and that predicted from the genomic sequence (*gene*) is shown *below*, of which only those amino acid residues differing from the cDNA-derived sequence are indicated. Amino acid residues are numbered to the *right*, beginning with the amino terminus. The positions of introns in the *CYP2A13* gene are also indicated. Only the carboxyl terminal half of the protein is shown. The nucleotide sequence of CYP2A13 cDNA has been assigned the GenBank accession no. AF209774.

Other Methods and Materials. Total RNA was prepared from frozen tissues according to the method of Chomczynski (34), with use of TRIzol Reagent (Life Technologies, Inc., Grand Island, NY). Preparation of heterologously expressed CYP2A6 in Sf9 cells was described previously (14). Protein concentrations were determined by the bicinchoninic acid method (Pierce, Rockford, IL) using BSA as the standard. Microsomal CYP was determined according to the procedure of Omura and Sato (35). CO-difference spectra of expressed CYP were recorded at room temperature using a Varian Model Cary 3E spectrometer. Polyclonal rabbit antibodies to CYP2A5 were prepared in a recent study (36). Immunoblot analysis was performed with an enhanced chemiluminescence kit from Amersham (Piscataway, NJ). Rabbit and rat NADPH-CYP reductase and rat b_5 were obtained as described previously (30, 31, 36).

RESULTS

cDNA Cloning and Sequence Verification. CYP2A mRNA expression was previously detected by RNA-blot analysis using CYP2A6 cDNA as a probe (5). The high degree of sequence similarity between CYP2A6 and CYP2A13 suggested that the detected signal might include transcripts from both isoforms. However, initial attempts using a RNA-PCR cloning strategy did not detect CYP2A13 mRNA in human liver.[4] In the present study, a similar PCR cloning strategy was used to identify and isolate CYP2A13 cDNA from human nasal mucosa. A total of 12 clones containing the PCR-amplified CYP2A13 coding region were isolated, all of which contained DNA inserts with identical restriction maps (data not shown). Three of the clones were completely sequenced and found to have identical nucleotide sequences, indicating that PCR errors did not occur. When the cDNA sequence was compared with the predicted coding nucleotide sequence of the previously reported *CYP2A13* genomic clones (1), eight nucleotide discrepancies were found, which resulted in seven amino acid substitutions, as shown in Fig. 1. The nucleotide differences between the gene and cDNA sequences are at (gene→cDNA, numbered from the translation start codon): 141 (C→G, exon 1, silent change), 624 (G→C, exon 4), 638 (G→C, exon 4), 1193 (A→T, exon 8), 1226 (A→G, exon 8), 1232 (G→T, exon 8), 1235 (G→A, exon 8), and 1255 (G→A, exon 8). However, in experiments not presented, DNA sequencing or RFLP analysis of the PCR products amplified from the exon 8 of the *CYP2A13* gene in 23 Chinese and 29 Caucasians detected only the nucleotide sequences corresponding to the cDNA, but not the genomic clones (1). Subsequently, an original *CYP2A13* genomic clone (no. 27292) was resequenced, and the results confirmed that the eight nucleotide differences represent sequencing errors in the published gene sequence, but not allelic variations. The silent nucleotide difference in exon 1 was also confirmed in a recent report (37) in which the CYP2A13 exon 1 sequence was obtained from a different genomic clone.

Characterization of Heterologously Expressed CYP2A13. A typical CYP CO-difference spectrum with an absorbance maximum at about 450 nm was recorded with detergent-solubilized microsomal preparations from CYP2A13-expressing Sf9 cells, as shown in Fig. 2. The peak at about 415 nm did not arise from P420 and was routinely detected in microsomal fractions from control Sf9 cells or cells infected with the wild-type virus, which did not show any CYP spectrum (not shown). The specific content of CYP in CYP2A13-expressing Sf9 microsomes ranged from 0.26 to 0.56 nmol of CYP/mg protein. Expression of the CYP2A13 protein was confirmed by immunoblot analysis with an antibody to mouse CYP2A5 (36). As shown in the inset of Fig. 2, a single band of the expected size was detected in the microsomal fraction of CYP2A13-expressing Sf9 cells, but not in control cells. The recombinant CYP2A13 migrated to the same position as did a CYP2A6 standard (not shown), suggesting that it was not degraded or posttranslationally modified.

The catalytic activities of CYP2A13 toward a number of known CYP2A6 substrates were examined in a reconstituted system. As shown in Table 1, although CYP2A13 was only about one-tenth as active as CYP2A6 in catalyzing coumarin 7-hydroxylation, it was as active as CYP2A6 toward DCBN and *N*-nitrosodiethylamine and 1.5- to 3.5-times more active than CYP2A6 toward *N*,*N*-dimethylaniline, *N*-nitrosomethylphenylamine, hexamethylphosphoramide, and 2′-methoxyacetophenone at 1 mM substrate concentrations.

The metabolic activity of CYP2A13 toward NNK, a major tobacco-specific nitrosamine and a potent respiratory carcinogen in animals, was then studied. HPLC analysis of [^{3}H]NNK metabolites formed during incubations with CYP2A13 indicated that the keto aldehyde was the major product and the keto alcohol was the minor product; no other metabolite peaks were detected (not shown). As shown in Table 2, CYP2A13 was much more active than CYP2A6 in the formation of both keto aldehyde and keto alcohol at an NNK concentration of 10 μM. The presence of sodium bisulfite in the incubation mixture to trap keto aldehyde (38) did not cause any inhibition of NNK metabolism catalyzed by either CYP2A6 or CYP2A13 (data not shown). The addition of b_5 slightly stimulated the activity of both enzymes, but CYP2A13 was still much more active than CYP2A6. Formation of the keto alcohol by CYP2A6 was not detectable at this substrate concentration. The same CYP2A13 and CYP2A6 preparations were also used to compare their metabolic activities toward MTBE, a gasoline

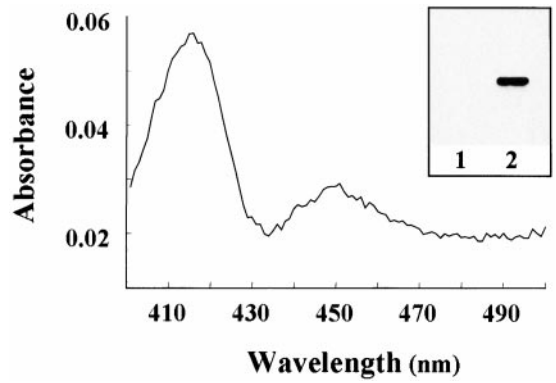

Fig. 2. CO-difference spectrum and immunoblot analysis of heterologously expressed CYP2A13. Microsomal preparations of CYP2A13-expressing Sf9 cells were solubilized with 0.5% Tergitol NP-10, and the spectrum was recorded at 22°C. *Inset*, immunoblot analysis of microsomal preparations (5 μg protein each) from control Sf9 cells and CYP2A13-expressing Sf9 cells, with a rabbit anti-mouse CYP2A5 antibody.

[4] J. Sheng and X. Ding, unpublished observations.

Table 1 *Catalytic activities of CYP2A13 and CYP2A6 toward xenobiotic compounds*

Reaction mixtures contained 50 mM phosphate buffer (pH 7.4), 1 mM NADPH, or an NADPH-generating system containing 0.4 mM NADP, 8.2 mM $MgCl_2$, 10 mM glucose-6-phosphate, and 0.4 units/ml glucose-6-phosphate dehydrogenase, a reconstituted CYP system containing 0.1 μM recombinant CYP in Sf9 microsomes and 0.3 μM-purified rabbit NADPH-CYP reductase, and a substrate at the indicated concentration. Reactions were carried out at 37°C for 20–50 min. The values presented, which are initial linear rates, are the average of duplicate determinations with differences <15% of the mean.

Substrate (concentration)	Reaction	Rate of product formation (nmol/min/nmol CYP)	
		CYP2A13	CYP2A6
Coumarin (0.1 mM)	7-Hydroxylation	0.26	2.2
2,6-Dichlorobenzonitrile (0.03 mM)	Protein adduct formation	0.04	0.03
N-Nitrosodiethylamine (1 mM)	*N*-Deethylation	0.81	0.58
Hexamethylphosphoramide (1 mM)	*N*-Demethylation	7.5	1.8
N,*N*-Dimethylaniline (1 mM)	*N*-Demethylation	8.0	2.0
2′-Methoxyacetophenone (1 mM)	*O*-Demethylation	7.2	1.6
N-Nitrosomethylphenylamine (1 mM)	*N*-Demethylation	10.6	4.3

Table 2 *Metabolism of NNK and MTBE by heterologously expressed human CYP2A6 and CYP2A13*

Metabolism of NNK and MTBE was assayed as described in "Materials and Methods." NNK (10 μM) and MTBE (0.25 mM) were incubated with the reconstituted CYPs at 37°C for 15 or 30 min, respectively. Where indicated, the molar ratio of CYP:b_5 was 1:4. The values reported are the average of two separate determinations with variations of <10% of the mean.

Enzyme	Rate of product formation (nmol/min/nmol CYP)		
	NNK		MTBE
	Keto aldehyde	Keto alcohol	*tert*-butyl alcohol
CYP2A13	1.8	0.45	1.1
CYP2A13 + b_5	2.2	0.62	1.4
CYP2A6	0.024	n.d.[a]	1.1
CYP2A6 + b_5	0.036	n.d.	1.1

[a] n.d., not detected.

ether that is a substrate of CYP2A6 (39). The activities of both CYP2A13 and CYP2A6 in the demethylation of MTBE were similar (Table 2).

Kinetic parameters of CYP2A13-catalyzed metabolic activation of NNK were subsequently determined in the presence of b_5 and with NNK concentrations ranging from 2 to 160 μM. As shown in Table 3, the apparent K_m value of CYP2A13 was 11.3 μM for the formation of keto aldehyde and 13.1 μM for the formation of keto alcohol. These K_m values are much lower than those of CYP2A6 or any other human CYP enzymes examined previously (21, 25). The catalytic efficiency, expressed as the ratio of V_{max}:K_m, of CYP2A13 was 29 and 44 times (for keto alcohol and keto aldehyde formation, respectively) higher than those found for CYP2A6 under similar conditions (25). These results indicate that CYP2A13 is a highly efficient enzyme for the metabolic activation of NNK.

Tissue Distribution of CYP2A13 mRNA. Specific antibodies against CYP2A13 are presently not available. Several anti-CYP2A antibodies, including anti-CYP2A10/11 (40), anti-CYP2A5 (36), and a monoclonal anti-CYP2A6 (Gentest), all recognized both CYP2A6 and CYP2A13 on immunoblots, and the two proteins were not resolved upon SDS-PAGE (data not shown). Therefore, it is presently difficult to determine the tissue distribution of CYP2A13 protein.

Consequently, tissue distribution of CYP2A13 mRNA was determined by RNA-PCR with isoform-specific primers. As shown in Fig. 3, a band of expected size for CYP2A13 (494 bp) was detected in liver, lung, nasal mucosa, and trachea, but not in heart or kidney. The lack of product in several tissues and in additional negative controls (not shown) in which RNA was omitted provided evidence that the PCR reaction was specific, *i.e.*, no cross-tissue contamination or nonspecific amplification occurred in these experiments. The CYP2A13 specificity of the primers was confirmed by direct sequencing of the PCR products, which did not reveal any sequences corresponding to CYP2A6 or CYP2A7 (All of the products sequenced were identical to 2A13; data not shown). In other experiments not shown, the same PCR product was also detected in brain, mammary gland, prostate, testis, and uterus, although at very low band intensity, but not in bone marrow, colon, small intestine, spleen, stomach, thymus, or skeletal muscle.

For those human tissues found to be positive for CYP2A13 mRNA expression by qualitative RNA-PCR, the relative levels of CYP2A13 and CYP2A6 mRNA were determined by competitive RNA-PCR. The efficiency of the RT step, as determined by the amount of product formed in competitive PCR from a constant amount of a modified cyclophilin transcript added to each RNA sample before the RT step, was about the same in various RNA samples used, with a maximal variation of <50%. The transcript level of endogenous cyclophilin, a housekeeping gene, was also determined in each RNA sample by competitive PCR, and was found to vary between 0.5×10^8 and 1.0×10^8 copy/μg total RNA among all samples tested, which confirmed the accuracy of the RNA concentrations determined spectrally. As shown in Table 4, the highest level of CYP2A13 was found in the nasal mucosa, which was 100 times higher than the CYP2A13 level in the liver and nearly 5 times as high as the level of CYP2A6 in the same tissue. On the other hand, CYP2A6 was found to have the highest level in the liver, almost 2000-fold higher than the level of CYP2A13 in the same tissue and about 16 times higher than CYP2A13 level in the nasal mucosa. The level of CYP2A13 mRNA was much lower in lung and trachea than in the nasal mucosa, but was still >10 times higher than in liver and 3–5 times higher than in testis (data not shown). The other positive tissues, including brain, uterus, prostate, and mammary gland, had CYP2A13 levels even lower than in the liver. In the lung, the level of CYP2A13 mRNA was about eight times higher than that of CYP2A6, and in the trachea, CYP2A13 was also more abundant than CYP2A6. Thus, in contrast to the previously

Table 3 *Kinetic parameters of NNK metabolism by CYP2A13 and comparison with published data for CYP2A6*

NNK metabolism was assayed as described in the legend to Table 2, with b_5 present. Reactions were carried out for lengths of time that allowed the determination of initial linear rates. The kinetic data for CYP2A13 were obtained from four separate experiments (mean ± SD). The data for CYP2A6 were from an earlier study (25) in which NNK metabolism was assayed using the enzyme expressed in baculovirus under conditions similar to that used here for CYP2A13 and also with the addition of b_5.

Product	CYP2A13			CYP2A6		
	K_m (μM)	V_{max} (nmol/min/nmol CYP)	V_{max}/K_m	K_m (μM)	V_{max} (nmol/min/nmol CYP)	V_{max}/K_m
Keto aldehyde	11.3 ± 3.5	4.1 ± 0.6	0.36	118	1.0	0.008
Keto alcohol	13.1 ± 5.1	1.2 ± 0.2	0.09	141	0.4	0.003

known liver-predominant expression of CYP2A6, CYP2A13 was preferentially expressed in the respiratory tract.

DISCUSSION

The present study clearly demonstrates that human CYP2A13 is functional, with facile activities toward many toxic chemicals that were previously shown to be substrates of CYP2A6. Furthermore, CYP2A13 mRNA is predominantly expressed in the respiratory tract. These results strongly suggest that CYP2A13 may play important roles in target tissue metabolic activation and in the toxicity of numerous xenobiotic compounds in the human respiratory system. Further studies on the characterization of the metabolic activities, identification of genetic polymorphisms, and determination of xenobiotic inducibility are under way. Results of these studies will provide valuable information to further elucidate the mechanism of tissue-selective xenobiotic toxicity in the human respiratory tract and may help with the design of chemoprevention strategies for respiratory cancer.

There is an inherent uncertainty associated with studying gene expression in autopsied or biopsied human samples in which the transcript levels are potentially influenced by individual differences in age, medical history, tissue preservation, and genetic polymorphism. In addition, the competitive RNA-PCR method is semiquantitative in nature. Nevertheless, the large differences in CYP2A13 mRNA levels observed between different tissues and the relative levels of CYP2A6 and CYP2A13 determined in the same RNA samples provide strong evidence that CYP2A13 is predominantly expressed in the respiratory tract and that, whereas CYP2A6 is a major CYP2A isoform in the liver, CYP2A13 is more abundant than CYP2A6 in the nasal mucosa and the lung. Previous immunohistochemical studies have detected abundant CYP2A-related proteins in human nasal mucosa; the immunoreactivity was localized to the supporting cells in the olfactory epithelium and acinar cells of Bowman's glands in the olfactory mucosa and in the ciliated epithelial cells and the serous gland acinar cells in the respiratory mucosa (4). The present finding that CYP2A13 mRNA is much more abundant than CYP2A6 mRNA in the nasal mucosa suggests that these CYP2A-immunoreactivities mainly represent CYP2A13, but not CYP2A6. However, it remains to be determined whether the two isoforms are located in different cellular populations or different regions in the nasal cavity. Thus, efforts to produce isoform-specific antibodies for additional immunocytochemical studies are warranted.

The detection of CYP2A13 in the human nasal mucosa was reported by Koskela *et al.* (7) during the preparation of this manuscript. These authors, using qualitative isoform-specific RNA-PCR, detected CYP2A13 in both liver and nasal mucosa. Although they did not quantify the mRNA levels of CYP2A13 in these two tissues and did not compare the relative mRNA levels of CYP2A6 and CYP2A13 in the nasal mucosa, their study did indicate that the level of CYP2A13 in the liver was below the limit of detection under conditions that allowed quantitative comparison of the levels of CYP2A6 and CYP2A7. This is consistent with the results from the present study indicating very low levels of CYP2A13 expression in the liver. Of interest, neither CYP2A6 nor CYP2A13 was detected in other human tissues examined by Koskela *et al.* (7), including the lung. The lack of detection of CYP2A6 in lung is in contrast to the present finding and previous reports on the detection of CYP2A6 in lung (8, 9).

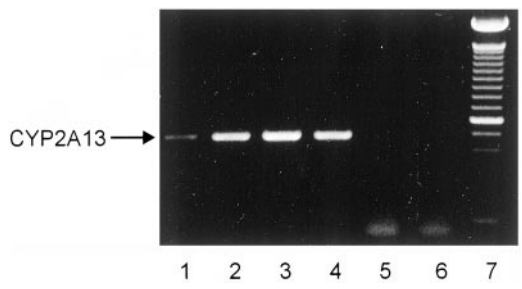

Fig. 3. Qualitative determination of the tissue distribution of CYP2A13 mRNA. CYP2A13 mRNA was detected by RNA-PCR with CYP2A13-specific primers as described in "Materials and Methods." The results of PCR analysis of the total RNAs from the liver (*Lane 1*), lung (*Lane 2*), nasal mucosa (*Lane 3*), trachea (*Lane 4*), heart (*Lane 5*), and kidney (*Lane 6*) are shown. DNA markers (100-bp ladder; *Lane 7*) were included for size determination. The position of the CYP2A13-derived PCR product is indicated.

Table 4 *Quantitative analysis of CYP2A13 and CYP2A6 mRNAs in human liver and respiratory tract tissues*

Levels of CYP2A13 and CYP2A6 mRNAs were determined individually by competitive RNA-PCR with use of isoform-specific PCR-mimics for quantification as described in "Materials and Methods." The results represent means ± SD, with the number of RNA samples analyzed for each tissue (*n*) indicated in parentheses, or the average of two determinations using a single RNA preparation of pooled tissues, with the individual values shown in parentheses. The total number of subjects whose tissues were used for RNA preparation, either pooled or individually, is also shown.

Tissue	Total no. of subjects	mRNA levels (attomoles/mg RNA)	
		CYP2A13	CYP2A6
Nasal mucosa	3	750 ± 210 (n = 3)	160 ± 140 (n = 3)
Liver	5	7 ± 6 (n = 4)	13000 ± 12000 (n = 4)
Lung	8	78 ± 32 (n = 4)	9 ± 1 (n = 4)
Trachea	84	130 (140, 120)	76 (74, 77)

Cigarette smoking is the single most important etiological factor of lung cancer (41, 42). NNK, which induces lung and nasal tumors in the rodents (43), is believed to play a significant role in the induction of lung cancer in smokers (44). The incidence of nasal tumors is also higher in smokers (45). Human liver and lung microsomes were both active in the metabolism of NNK; the activities were significantly inhibited by carbon monoxide, which is consistent with CYP involvement (21). The major CYP isoform(s) responsible for NNK activation in human target tissues have not been identified. An earlier study indicated that CYP2E1 and CYP2A6 are major catalysts for activation of NNK in human liver microsomes (46). Antibodies and inhibitors to CYP1A and CYP2E1 inhibited metabolic activation in liver, but not in lung, whereas antibodies to CYP2A1, 2C8, 2D1, or 3A4 had little or no effect on the metabolism of NNK in either tissue (21). NNK can be activated by CYP2A6 to form DNA adducts (47). In lung microsomes, CYP2A6 or a related enzyme was implicated in the activation, and lipoxygenases and lipid hydroperoxides possibly also were involved (22). Thus, the present finding that CYP2A13 is much more active than CYP2A6 and other human CYPs in the activation of NNK is of particular interest.

In conclusion, we demonstrated that among all of the human CYP enzymes examined thus far, CYP2A13 is the most active form, with the highest efficiency, for the metabolic activation of NNK. Together with its predominant expression in the nasal mucosa and lung, we hypothesize that CYP2A13 may play an important role in tobacco-related tumorigenesis in human respiratory tract.

ACKNOWLEDGMENTS

We thank Dr. Harvey Mohrenweiser of Lawrence Livermore National Laboratory (Livermore, CA) for providing the *CYP2A13* genomic clone no. 27292, Drs. Simon Spivack and Robert Jansing of the Wadsworth Center (Albany, NY) for providing human lung and liver tissues, respectively, and Drs. Laurence Kaminsky and Katherine Henrikson for reading the manuscript. We also gratefully acknowledge the use of the Biochemistry, Molecular Genetics, Molecular Immunology, and Tissue Culture Core Facilities of the Wadsworth Center.

REFERENCES

1. Fernandez-Salguero, P., Hoffman, S. M., Cholerton, S., Mohrenweiser, H., Raunio, H., Rautio, A., Pelkonen, O., Huang, J. D., Evans, W. E., Idle, J. R., and Gonzalez, F. J. A genetic polymorphism in coumarin 7-hydroxylation: sequence of the human *CYP2A* genes and identification of variant *CYP2A6* alleles. Am. J. Hum. Genet., *57:* 651–660, 1995.
2. Yun, C. H., Shimada, T., and Guengerich, F. P. Purification and characterization of human liver microsomal cytochrome P-450 2A6. Mol. Pharmacol., *40:* 679–685, 1991.
3. Maurice, M., Emiliani, S., Dalet-Beluche, I., Derancourt, J., and Lange, R. Isolation and characterization of a cytochrome P450 of the IIA subfamily from human liver microsomes. Eur. J. Biochem., *200:* 511–517, 1991.
4. Getchell, M. L., Chen, Y., Ding, X., Sparks, D. L., and Getchell, T. V. Immunohistochemical localization of a cytochrome P-450 isozyme in human nasal mucosa: age-related trends. Ann. Otol. Rhinol. Laryngol., *102:* 368–374, 1993.
5. Su, T., Sheng, J. J., Lipinskas, T. W., and Ding, X. Expression of *CYP2A* genes in rodent and human nasal mucosa. Drug Metab. Dispos., *24:* 884–890, 1996.
6. Thornton-Manning, J. R., Nikula, K. J., Hotchkiss, J. A., Avila, K. J., Rohrbacher, K. D., Ding, X., and Dahl, A. R. Nasal cytochrome P450 2A: identification, regional localization, and metabolic activity toward hexamethylphosphoramide, a known nasal carcinogen. Toxicol. Appl. Pharmacol., *142:* 22–30, 1997.
7. Koskela, S., Hakkola, J., Hukkanen, J., Pelkonen, O., Sorri, M., Saranen, A., Anttila, S., Fernandez-Salguero, P., Gonzalez, F., and Raunio, H. Expression of *CYP2A* genes in human liver and extrahepatic tissues. Biochem. Pharmacol., *57:* 1407–1413, 1999.
8. Shimada, T., Yamazaki, H., Mimura, M., Wakamiya, N., Ueng, Y. F., Guengerich, F. P., and Inui, Y. Characterization of microsomal cytochrome P450 enzymes involved in the oxidation of xenobiotic chemicals in human fetal liver and adult lungs. Drug Metab. Dispos., *24:* 515–522, 1996.
9. Crawford, E. L., Weaver, D. A., Demuth, J. P., Jackson, D. M., Khuder, S. A., Frampton, M. W., Utell, M. J., Thilly, W. G., and Willey, J. C. Measurement of cytochrome P450 *2A6* and *2E1* gene expression in primary human bronchial epithelial cells. Carcinogenesis (Lond.), *19:* 1867–1871, 1998.
10. Mace, K., Bowman, E. D., Vautravers, P., Shields, P. G., Harris, C. C., and Pfeifer, A. M. A. Characterisation of xenobiotic-metabolising enzyme expression in human bronchial mucosa and peripheral lung tissues. Eur. J. Cancer, *34:* 914–920, 1998.
11. Fernandez-Salguero, P., and Gonzalez, F. J. The *CYP2A* gene subfamily: species differences, regulation, catalytic activities and role in chemical carcinogenesis. Pharmacogenetics, *5:* S123–S128, 1995.
12. Messina, E. S., Tyndale, R. F., and Sellers, E. M. A major role for CYP2A6 in nicotine C-oxidation by human liver microsomes. J. Pharmacol. Exp. Ther., *282:* 1608–1614, 1997.
13. Yamazaki, H., Inoue, K., Hashimoto, M., and Shimada, T. Roles of CYP2A6 and CYP2B6 in nicotine C-oxidation by human liver microsomes. Arch. Toxicol., *73:* 65–70, 1999.
14. Liu, C., Zhuo, X., Gonzalez, F. J., and Ding, X. Baculovirus-mediated expression and characterization of rat CYP2A3 and human CYP2A6: role in metabolic activation of nasal toxicants. Mol. Pharmacol., *50:* 781–788, 1996.
15. Patten, C. J., Smith, T. J., Friesen, M. J., Tynes, R. E., Yang, C. S., and Murphy, S. E. Evidence for cytochrome P450 2A6 and 3A4 as major catalysts for N′-nitrosonornicotine α-hydroxylation by human liver microsomes. Carcinogenesis (Lond.), *18:* 1623–1630, 1997.
16. Miyamoto, M., Umetsu, Y., Dosaka-Akita, H., Sawamura, Y., Yokota, J., Kunitoh, H., Nemoto, N., Sato, K., Ariyoshi, N., and Kamataki, T. *CYP2A6* gene deletion reduces susceptibility to lung cancer. Biochem. Biophys. Res. Commun., *261:* 658–660, 1999.
17. Yamano, S., Tatsuno, J., and Gonzalez, F. J. The *CYP2A3* gene product catalyzes coumarin 7-hydroxylation in human liver microsomes. Biochemistry, *29:* 1322–1329, 1990.
18. Ding, S., Lake, B. G., Friedberg, T., and Wolf, C. R. Expression and alternative splicing of the cytochrome P-450 CYP2A7. Biochem. J., *306:* 161–166, 1995.
19. Hecht, S. S. Tobacco smoke carcinogens and lung cancer. J. Natl. Cancer Inst., *91:* 1194–1210, 1999.
20. Hecht, S. S. Biochemistry, biology and carcinogenicity of tobacco-specific *N*-nitrosamines. Chem. Res. Toxicol., *11:* 559–603, 1998.
21. Smith, T. J., Guo, Z., Gonzalez, F. J., Guengerich, F. P., Stoner, G. D., and Yang, C. S. Metabolism of 4-(methylnitrosamino)-1-(3-pyridyl)-1-butanone in human lung and liver microsomes and cytochromes P-450 expressed in hepatoma cells. Cancer Res., *52:* 1757–1763, 1992.
22. Smith, T. J., Stoner, G. D., and Yang, C. S. Activation of 4-(methylnitrosamino)-1-(3-pyridyl)-1-butanone (NNK) in human lung microsomes by cytochromes P450, lipoxygenase, and hydroperoxides. Cancer Res., *55:* 5566–5573, 1995.
23. Smith, T. J., Guo, Z., Guengerich, F. P., and Yang, C. S. Metabolism of 4-(methylnitrosamino)-1-(3-pyridyl)-1-butanone (NNK) by human cytochrome P450 1A2 and its inhibition by phenethyl isothiocyanate. Carcinogenesis (Lond.), *17:* 809–813, 1996.
24. Penman, B. W., Reece, J., Smith, T., Yang, C. S., Gelboin, H. V., Gonzalez, F. J., and Crespi, C. L. Characterization of a human cell line expressing high levels of cDNA-derived CYP2D6. Pharmacogenetics, *3:* 28–39, 1993.
25. Patten, C. J., Smith, T. J., Murphy, S. E., Wang, M. H., Lee, J., Tynes, R. E., Koch, P., and Yang, C. S. Kinetic analysis of the activation of 4-(methylnitrosamino)-1-(3-pyridyl)-1-butanone by heterologously expressed human P450 enzymes and the effect of P450-specific chemical inhibitors on this activation in human liver microsomes. Arch. Biochem. Biophys., *333:* 127–138, 1996.
26. Nash, T. The colorimetric estimation of formaldehyde by means of the Hantzsch reaction. Biochem. J., *55:* 416–421, 1953.
27. Greenlee, W. F., and Poland, A. An improved assay of 7-ethoxycoumarin O-deethylase activity: induction of hepatic enzyme activity in C57BL/6J and DBA/2J mice by phenobarbital, 3-methylcholanthrene and 2,3,7,8-tetrachlorodibenzo-p-dioxin. J. Pharmacol. Exp. Ther., *205:* 596–605, 1978.
28. Ding, X., Spink, D. C., Bhama, J. K., Sheng, J. J., Vaz, A. D., and Coon, M. J. Metabolic activation of 2,6-dichlorobenzonitrile, an olfactory-specific toxicant, by rat, rabbit, and human cytochromes P450. Mol. Pharmacol., *49:* 1113–1121, 1996.
29. Yoo, J. S., Guengerich, F. P., and Yang, C. S. Metabolism of *N*-nitrosodialkylamines by human liver microsomes. Cancer Res., *48:* 1499–1504, 1988.
30. Hong, J. Y., Wang, Y. Y., Bondoc, F. Y., Yang, C. S., Lee, M. J., and Huang, W. Q. Rat olfactory mucosa displays a high activity in metabolizing methyl tert-butyl ether and other gasoline ethers. Fundam. Appl. Toxicol., *40:* 205–210, 1997.
31. Hong, J. Y., Yang, C. S., Lee, M., Wang, Y. Y., Huang, W. Q., Tan, Y., Patten, C. J., and Bondoc, F. Y. Role of cytochromes P450 in the metabolism of methyl tert-butyl ether in human livers. Arch. Toxicol., *71:* 266–269, 1997.
32. Smith, T. J., Guo, Z-Y., Thomas, P. E., Chung, F-L., Morse, M. A., Eklind, K., and Yang, C. S. Metabolism of 4-(methylnitrosamino)-1-(3-pyridyl)-1-butanone in mouse lung microsomes and its inhibition by isothiocyanates. Cancer Res., *50:* 6817–6822, 1990.
33. Guo, Z., Smith, T. J., Thomas, P. E., and Yang, C. S. Metabolism of 4-(methylnitrosamino)-1-(3-pyridyl)-1-butanone (NNK) by inducible and constitutive cytochrome P450 enzymes in rats. Arch. Biochem. Biophys., *298:* 279–286, 1992.
34. Chomczynski, P. A reagent for the single-step simultaneous isolation of RNA, DNA and proteins from cell and tissue samples. Biotechniques, *15:* 532–534, 1993.
35. Omura, T., and Sato, R. The carbon monoxide-binding protein of liver microsomes. I. Evidence for its hemoprotein nature. J. Biol. Chem., *239:* 2370–2378, 1964.
36. Gu, J., Zhang, Q-Y., Genter, M. B., Lipinskas, T. W., Negishi, M., Nebert, D. W., and Ding, X. Purification and characterization of heterologously expressed mouse CYP2A5 and CYP2G1—role in metabolic activation of acetaminophen and 2,6-dichlorobenzonitrile in mouse olfactory mucosal microsomes. J. Pharmacol. Exp. Ther., *285:* 1287–1295, 1998.
37. Nunoya, K., Yokoi, T., Kimura, K., Kainuma, T., Satoh, K., Kinoshita, M., and Kamataki, T. A new *CYP2A6* gene deletion responsible for the *in vivo* polymorphic metabolism of (+)-cis-3,5-dimethyl-2-(3-pyridyl)thiazolidin-4-one hydrochloride in humans. J. Pharmacol. Exp. Ther., *289:* 437–442, 1999.
38. Peterson, L. A., Mathew, R., and Hecht, S. S. Quantitation of microsomal α-hydroxylation of the tobacco-specific nitrosamine, 4-(methylnitrosamino)-1-(3-pyridyl)-1-butanone. Cancer Res., *51:* 5495–5500, 1991.
39. Hong, J. Y., Wang, Y. Y., Bondoc, F. Y., Lee, M., Yang, C. S., Hu, W. Y., and Pan, J. M. Metabolism of methyl tert-butyl ether and other gasoline ethers by human liver microsomes and heterologously expressed human cytochromes P450: identification of *CYP2A6* as a major catalyst. Toxicol. Appl. Pharmacol., *160:* 43–48, 1999.
40. Ding, X., and Coon, M. J. Immunochemical characterization of multiple forms of cytochrome P-450 in rabbit nasal microsomes and evidence for tissue-specific expression of P-450s NMa and NMb. Mol. Pharmacol., *37:* 489–496, 1990.
41. Hoffmann, D., Brunnemann, K. D., Prokopczyk, B., and Djordjevic, M. V. Tobacco-specific *N*-nitrosamines, and Areca-derived *N*-nitrosamines: chemistry, biochemistry, carcinogenicity, and relevance to humans. J. Toxicol. Environ. Health, *41:* 1–52, 1994.
42. Spivack, S. D., Fasco, M. J., Walker, V. E., and Kaminsky, L. S. The molecular epidemiology of lung cancer. Crit. Rev. Toxicol., *27:* 319–365, 1997.
43. Hecht, S. S., Chen, C. B., Ohmori, T., and Hoffmann, D. Comparative carcinogenicity in F344 rats of the tobacco-specific nitrosamines, *N*′-nitrosonornicotine and 4-(*N*-methyl-*N*-nitrosamino)-1-(3-pyridyl)-1-butanone. Cancer Res., *40:* 298–302, 1980.
44. Hecht, S. S. Approaches to cancer prevention based on an understanding of *N*-nitrosamine carcinogenesis. Proc. Soc. Exp. Biol. Med., *216:* 181–191, 1997.
45. Ayiomamitis, A., Parker, L., and Havas, T. The epidemiology of malignant neoplasms of the nasal cavities, the paranasal sinuses and the middle ear in Canada. Arch. Oto-Rhino-Laryngol., *244:* 367–371, 1988.
46. Yamazaki, H., Inui, Y., Yun, C. H., Guengerich, F. P., and Shimada, T. Cytochrome P450 2E1 and 2A6 enzymes as major catalysts for metabolic activation of *N*-nitrosodialkylamines and tobacco-related nitrosamines in human liver microsomes. Carcinogenesis (Lond.), *13:* 1789–1794, 1992.
47. Tiano, H. F., Wang, R. L., Hosokawa, M., Crespi, C., Tindall, K. R., and Langenbach, R. Human CYP2A6 activation of 4-(methylnitrosamino)-1-(3-pyridyl)-1-butanone (NNK): mutational specificity in the *gpt* gene of AS52 cells. Carcinogenesis (Lond.), *15:* 2859–2866, 1994.